Primary Frequency Control Using Motor Drives for Short Term Grid Disturbances

Taylor L. Short, Shuyao Wang, Leon M. Tolbert, Jingxin Wang, Yiwei Ma, Yunting Liu, Fred Wang

***Abstract*—Industrial motor systems make up a quarter of all electric sales in the United States. Variable speed drives (VSDs) can provide energy efficiency savings to the customer by regulating motor speed based on specific and varying needs. In addition to the benefits provided to the customer, VSDs can provide support to the grid through ancillary services. The Center for Ultra-Wide-Area Resilient Electric Energy Transmission Networks (CURENT) developed a power electronics converter-based grid emulator to allow testing of various power system architectures and demonstration of key technologies in monitoring, control, actuation, and visualization. This paper proposes using an active front-end VSD's connected motor load to provide frequency regulation to a large scale power grid. Each part of the emulator is described including motor and power electronics model and control. The proposed frequency regulation is implemented in VSDs and modeled in both a transmission system in EMTDC/PSCAD and verified on CURENT's hardware testbed.**

I. Introduction

INDUSTRIAL induction motors are considered the workhorse for industry because of their low cost and robust construction. Induction motors are used in a wide range of industries, such as oil, mining, power, marine, paper, and wastewater. Applications include fans, pumps, compressors, grinding mills, metal rolling, mine hoists, refiners, and propulsion. An induction motor can be connected directly to the 60 Hz power grid and will operate at a relatively constant speed. Motor drives consist of two conversion phases– AC to DC and DC to AC or rectifier and inverter respectively. The rectifier and inverter are connected by a DC link capacitor. See Fig. 1 for an example of a basic motor drive topology. The motor drive consists of two parts: the inverter and the rectifier. The inverter and rectifier are connected through a DC capacitor link. The three-phase AC side of the inverter is connected to the motor load, and the three-phase AC side of the rectifier is connected to the three-phase power grid. Most motor drive systems are referred to as adjustable speed drives (ASDs) or variable speed drives (VSDs).

A. Motor Drives Benefits and Advantages

According to a study done by the International Energy Agency in 2011, 64% of all electric consumption is industrial motor loads. Large electric motors with more than 375 kW output power make up about 23% of all motor power consumption [1]. According to an assessment done by DOE in 2002, only 8% of all industrial motor systems have variable speed drives (VSDs). However, in this same study, it was determined that nearly two-thirds of all potential energy

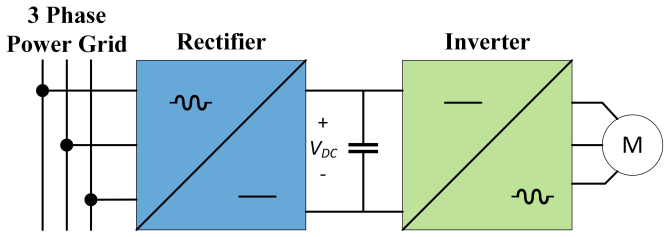

Fig. 1. Motor drive basic schematic.

efficiency savings set forth by the Consortium for Energy Efficiency are accomplished by system improvements, such as VSDs or bypass loops in pumping systems [2]. Pumps, fans, and compressors show considerable efficiency improvements when VSDs are implemented. A VSD can regulate the flow of water or gas without the use of traditional mechanical equipment, which introduce significant loss into the system [3].

The survey suggests that a conservative estimate for energy savings from a VSD is 787 GWh/year for fan systems, 1366 GWh/year for air systems, and 6421 GWh/year for pump systems. The mid-range estimates for these savings are nearly twice that of the conservative estimates [2].

As of 2002, while 8% of industrial motor systems were equipped with a VSD, 90% of those were 20 hp or less. However, DOE estimated that 18-25% of total manufacturing motor system energy could add VSDs cost effectively [2]. The average payback time-frame on the investment of VSDs is only a year and a half. In addition to an increase in energy efficiency, VSDs lower starting currents and can effectively regulate the speed and power at or below nominal ratings [4] [5]. Inherent drawbacks of VSDs are the PWM voltage change (switching action) effect on motors because the multiple, rapid dV/dt produced by inverters can result in causing bearing currents or lead to motor winding insulation breakdown; however, motor manufacturers have modified motor designs such that they can reliably run with front-end VSDs.

In addition to energy efficiency savings, a VSD-connected motor can provide potential benefits to the grid. The same reduction of the inrush current also improves stability of the power grid during motor startup [4]. Additionally, loads such as fans, air compressors, and pumps can be controlled to provide support to the power grid, which are the same systems that find the majority of energy efficiency benefits from VSDs. The speed of (and power drawn from the utility) fans, air compressors and pumps can often be reduced without affecting the primary production process. These loads make up

roughly 11% of all industrial motor loads [2]. This is a huge untapped resource for utilities. These loads could respond to grid fluctuations and assist in making the grid more reliable.

Load-side participation in frequency regulation provides possible advantages in faster response, lower fuel consumption and emission, and better localization of disturbances [6]. VSDs are particularly equipped to implement frequency regulation, because load can be changed by changing motor speed. This is unique; most loads are controlled to be either on or off [7]. Whereas the availability of ancillary services is more unpredictable from loads than from traditional ancillary service sources such as those provided by distributed generation, the development of VSDs and the increase in energy prices may provide an opening for load side participation into the regulation market [8].

B. Ancillary Services

Ancillary services can support basic grid functions such as generating capacity, energy supply, and power delivery. This support is often provided by distributed energy resources (DER) or distributed generation (DG). However, with the integration of power electronic interfaced loads, many of the support functions provided by DG ancillary services can also be provided by flexible loads. Currently, independent system operators' requirements do not allow much room for loads to operate in the regulatory market. For example, California Independent System Operators (CAISO) requires at least 0.5 MW power capacity to be able to participate in the frequency regulation market [9]. The focus of most interest in flexible loads is centered around air conditioning units and other residential loads. However, a medium voltage motor can have an operating capacity of near 5 MW, allowing a larger controllable capacity.

By 2009, both New York Independent System Operator (NYISO) and PJM Interconnect LLC (PJM) had a demand side ancillary service program [10]. For NYISO, demand side resources could participate in regulation and synchronous and non-synchronous reserve. PJM allows participation in regulation, synchronous reserve, and day ahead scheduling reserves [10].

The use of loads to regulate the grid is referred to as demand response. Most demand response programs adjust the load by an ON or OFF option. This happens one of two ways: (1) the customer gives the utility permission to interrupt their load during a designated time or (2) the customer is incentivised to reduce load during a time period. However, with the introduction of VSDs, loads' speed– and therefore load– can be varied over time. Large industrial fans and pumps are especially advantageous for this application because these loads can often be reduced for a short time and will not interrupt any production processes.

There are two major regulatory services that can be provided by industrial VSDs: frequency regulation and voltage regulation. This paper focuses on frequency regulation. Frequency regulation provides active power or absorbs active power depending on the grid frequency. If the frequency is above the reference value, active power from the load is increased.

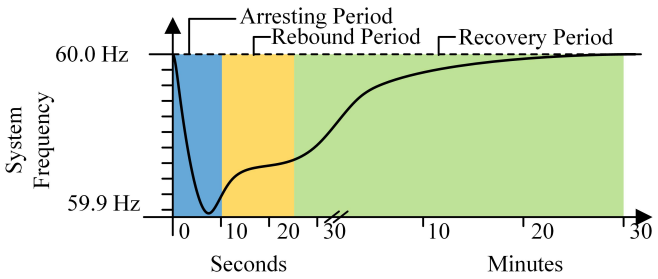

Fig. 2. A sudden drop in system frequency triggers automated response to correct the frequency, followed by manual interventions from power system operators. Ancillary services provide these responses [11].

If frequency is below the reference value, active power from the load is reduced. Primary frequency regulation happens within 30 seconds of the initial frequency fluctuation. After 30 seconds, generation secondary control takes over regulation. Fig. 2 shows the typical response for frequency regulation.

C. Grid Frequency Support Using Variable Motor Speed

Adjustable speed drives are generally controlled using constant V/f control [12]. Using this method of control, the power from the motor can be reduced by reducing the motor speed. The inertia response of a line connected motor is emulated using the frequency response control. However, this control adds the primary frequency control. The frequency control reference in [12] uses a phase-lock loop (PLL) to measure the grid frequency. The grid frequency and the initial motor speed are the inputs for the system. The control scheme is shown in Fig. 3. The control includes primary frequency control (Fig. 3(a)), inertia emulator (Fig. 3(b)), and the speed controller (Fig. 3(c)). f_{grid} is the PLL measured value for the grid frequency, R_l refers to the droop gain, $\omega_{r,ref}$ is the pre-event motor reference speed, and C_1 and C_2 are coefficients based on induction motor parameters [13]. Some common values for C_1 and C_2 are shown in Table I. The time constants for the primary frequency control LPF and the inertia emulator LPF are set to 1 s and 0.1 s, respectively.

TABLE I. Derived coefficients for induction motors [13].

Motor Type	Ventilation	Small Industrial	Large Industrial
C_1	0.86268	0.96761	0.99653
C_2	0.10306	0.03777	0.01201

Another method for grid frequency support is inertia emulation using the DC voltage link in the VSD. This is a method commonly used for wind turbines or multi-terminal HVDC (MTDC) systems [14]. In this method when used for MTDC, both the electric energy stored in the DC link capacitors and the energy transferred from the remote grid side to the main AC transmission grid are used to regulate the grid frequency. This control method is shown in Fig. 4. The $V_{dc,ref}$ changes according to the deviation of the grid frequency, which can be expressed in (1):

$$K_c \cdot (f_{meas} - f_{nom}) + V_{dc,nom} = V_{dc,ref} \qquad (1)$$

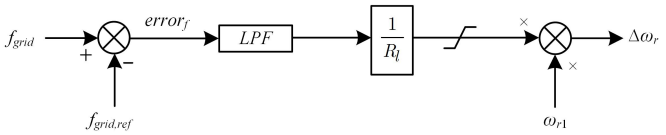

(a) Primary controller.

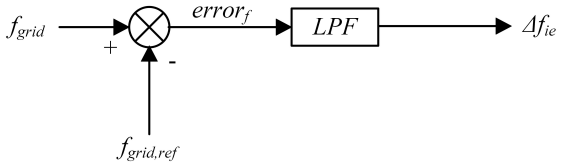

(b) Inertia emulator.

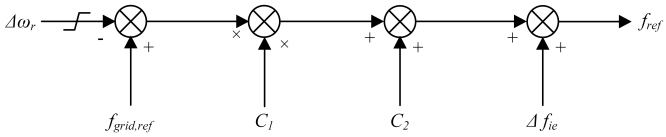

(c) Speed controller.

Fig. 3. The block diagram of the primary controller 3(a), inertia emulator 3(b), and the speed controller 3(c) [12].

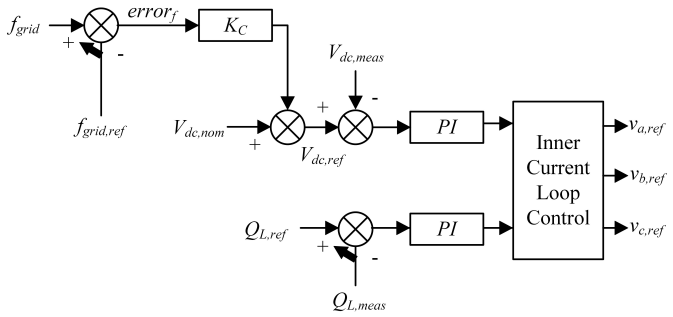

Fig. 4. VSC inertia emulation control [14].

where K_c is the proportional control parameter of the voltage source converter (VSC), f_{nom} is the initial frequency reference, f_{meas} is the real time grid frequency, and $V_{dc,nom}$ is the initial DC link voltage reference. The active power contribution of the DC link capacitor after a grid disturbance can be expressed in (2):

$$\Delta P_{VSC}(p.u.) = \frac{NCV_{dc,nom}}{S_{VSC}} \cdot \frac{dV_{dc,ref}}{dt} = \frac{NK_cCV_{dc,nom}}{S_{VSC}} \cdot \frac{df_{meas}}{dt} \quad (2)$$

where N is the number of the DC link capacitors, C is the capacitance of each dc link capacitor, S_{VSC} is the rated power of the VSC. For a 2.5 kW motor, the K_C would be optimized to 77.16 and the LPF would be set at 30 Hz [14].

D. Hardware Testbed

The Center for Ultra-Wide-Area Resilient Electric Energy Transmission Networks (CURENT) developed a power electronics converter-based grid emulator, known as the Hardware Testbed (HTB), to allow testing of various power system architectures and demonstration of key technologies in monitoring, control, actuation, and visualization [15]. Using reconfigurable voltage source inverters, the HTB emulates interconnected generation and loads. The HTB is designed with the converters connected to a DC bus on one side and the AC grid emulation on the other, as shown in Fig. 5. The DC link is supplied by the real power grid through a transformer and an active rectifier. The power flows from the DC link to the AC grid emulation for the generator emulators and from the AC grid emulation to the DC link for the load emulators.

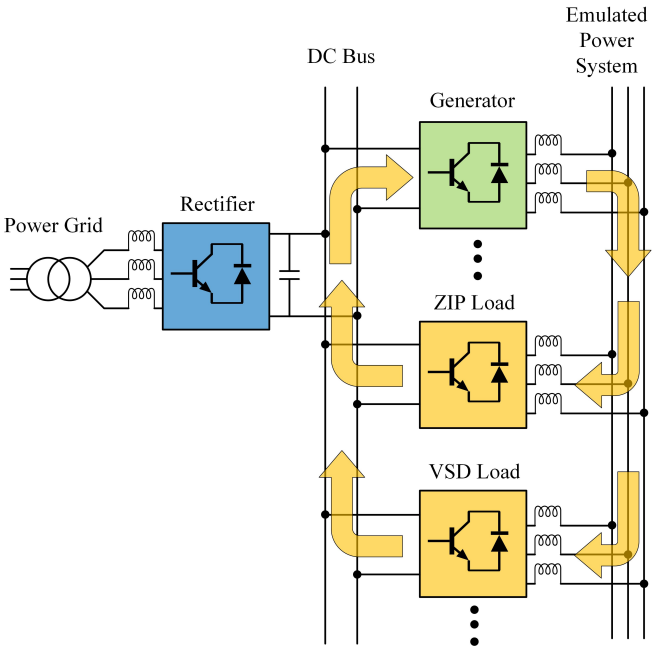

Fig. 5. Power circulation within the HTB [20].

Converter based emulators can be designed to have a bandwidth of several kHz, which allows the converters to accurately emulate voltage and current dynamics of the actual power system components. The HTB emulates the resiliency of the system by incorporating real time communication, protection, control, and cybersecurity; and it has the capability to examine many scenarios including line and bus faults [16] [17] [18] [19]. The HTB and PSCAD are used to evaluate the model and grid system response.

The structure of the paper is organized as follows: Section II introduces the topology, modeling for VSD, and the grid frequency regulation control. Section III-A provides the experimental results on the HTB platform that verify the VSD model. Section III-B presents multiple scenarios tested in EMTDC/PSCAD using the frequency support provided by the VSD model.

II. Load Modeling for the Power Emulator on the HTB

The electrical topology shown in Fig. 6 was chosen for the VSD and induction motor emulator. The implementation of active front-end (AFE) has become increasingly popular

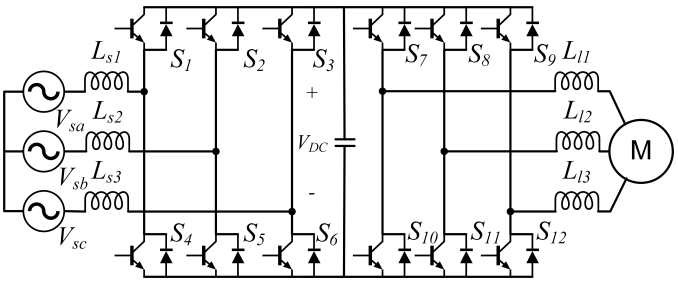

Fig. 6. Active front end motor drive topology for emulation.

because of the decreasing cost of power switches [21]. AFE-VSDs draw near sinusoidal line current with less harmonic distortion compared with that of the diode front-end (DFE) VSDs. In addition to reducing the harmonic distortion, AFE-VSDs allow for more control and for grid regulation. The inverter can control the motor, and rectifier controls provide grid support. AFE-VSDs are becoming the standard solution for large-power medium-voltage VSDs [22]. While AFE has some benefits compared to DFE, there are some disadvantages, including complicated control, potential resonance, and bulky and expensive LCL filter [23]. However, given the control flexibility and reduction of line harmonics, an AFE-VSD topology is the focus of this study.

Each emulator on the HTB has the same inner current loop for the VSI, using a basic PI current control. In this case, $i_{d,ref}$ and $i_{q,ref}$ are the calculated reference values from the active front-end VSD. The final output of the emulator is the duty cycle reference for the HTB VSI. DC voltage control is implemented in the rectifier, and grid frequency control is implemented in the inverter of the VSD.

A three-phase induction motor is the dominant power system load, particularly for industrial systems. An accurate emulator should include dynamic behaviors in order to emulate overall power system behaviors. References [20] and [24] outline the model used for the HTB emulation. The values for the induction motor used in this emulation are shown in Table II.

The VSD design uses an active front-end VSD topology, shown in Fig. 6. Table II shows the base values for the VSD emulator. These values were based on a commercial medium voltage motor and the corresponding values for a VSD rated for a motor of that size. The back end of a VSD is connected to the induction motor load and can be modeled by a voltage source inverter (VSI). The average model for VSD including the rectifier and VSI is shown in Fig. 7 [25].

TABLE II. Values for designed VSD and motor emulation.

Variable	Emulation value	Variable	Emulation value
X_{lr}	0.0916 p.u.	r_s	0.0104 p.u.
X_{ls}	0.061 p.u.	$V_{dc,ref}$	9 kV
X_m	2.11 p.u.	P_{base}	3 MW
X_{rr}	2.2 p.u.	$V_{LL,base}$	4.16 kV
X_{ss}	2.1696 p.u.	C_{dc}	6.4 mF
r_r	0.0076 p.u.	f_{sw}	5 kHz

For an active front end VSD, the DC voltage control is done in the rectifier. The DC link voltage control isolates the grid

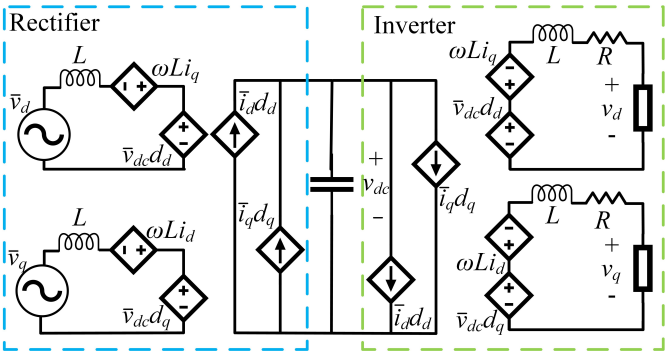

Fig. 7. Average model of VSD in dq coordinates [25].

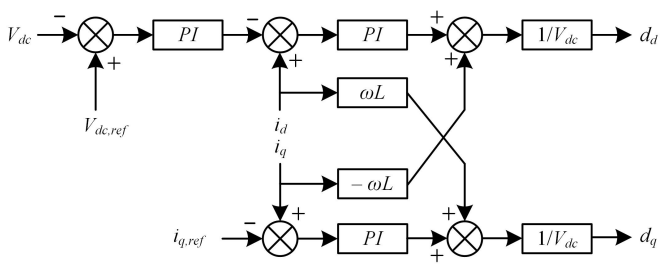

Fig. 8. DC link voltage control [26].

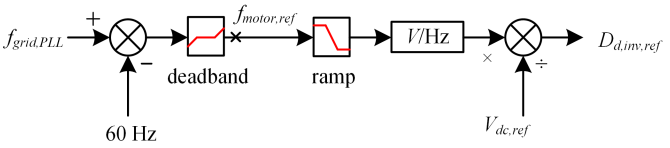

(a) Determination of motor reference $f_{motor,ref}$ based on the grid frequency

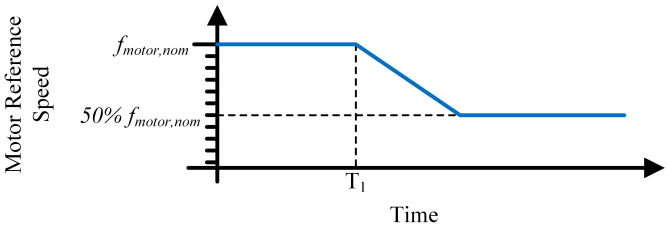

(b) $f_{motor,ref}$ related to when grid frequency: at $t = T_1$, grid frequency goes below the deadband.

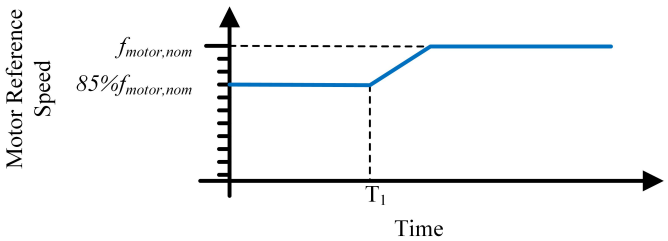

(c) $f_{motor,ref}$ related to when grid frequency: at $t = T_1$, grid frequency goes above the deadband.

Fig. 9. VSD frequency regulation control.

voltage from the motor output voltage. This emulator uses a basic PI control, shown in Fig. 8 [26]. Using the average model, shown in Fig. 7, the PI parameters were designed using Matlab/Simulink.

A. Motor Constant V/f Control

Constant V/f control is an open loop control scheme, widely used because of its cost-effectiveness. It is a cost effective technique because: (1) an advanced microprocessor is not needed, and (2) there are less electrical sensors needed to feed back information to the control. Constant V/f control is used to change voltage at the terminal of the induction motor proportionally to the change of motor reference speed [27], i.e.,

$$V_{dinv,ref} = \frac{V_{nom}}{f_{nom}} \cdot f_{ref} \tag{3}$$

where $V_{dinv,ref}$ is the output reference voltage for the inverter and f_{ref} is the desired frequency of the motor.

The value of V_{nom} and f_{nom} are set to 1 p.u., because all emulator controls are done in per unit values. Therefore, in the per unit system the control is simplified to:

$$V_{dinv,ref} = f_{ref} \tag{4}$$

B. Grid Frequency Regulation Transmission System

The frequency regulation for the transmission system simply reduces or increases the load based on the value of the grid frequency error. The motor frequency reference is limited to 50% to 100% of the nominal operating speed, and a response is triggered when the measured error of the grid frequency goes outside the deadband of $\pm$60 mHz. The grid frequency regulation can run for a maximum of 30 seconds, after which the speed ramps back to the nominal value at a rate of 3%/ second.

Fig. 9 describes the VSD control used for the grid frequency regulation. As illustrated in Fig. 9(a), the control uses the change in grid frequency to trigger the motor reference speed to ramp to 50% of the nominal value, when the grid frequency goes outside the deadband of 60 mHz. Since this ramp is achieved with an open loop V/Hz control, the ramp rate must be limited to ensure the ramp rate is achievable and reliable. A fast ramp rate could cause a loss of control or may not be achievable with this design. In this case, a 10 Hz/s motor ramp speed is chosen to minimize negative affects to the motor, while proving significant grid support. The motor speed will ramp back to its nominal speed, when either the grid frequency goes above the deadband, or the frequency regulation has run for 30 seconds. The relation between the grid frequency and $f_{motor,ref}$ explained above is illustrated in Fig. 9(b). Fig. 9(c) shows the case when the grid frequency goes above the deadband of 60 mHz. For example, if there was a line loss on the grid, grid frequency would increase above the specified deadband. For this case, the motor speed was assumed to be at 85% of the maximum value. Such control scheme was chosen because it limits the effect on the load, while maximizing the benefit to the grid.

Due to the variability of frequency on a transmission grid, a proportional (P) or proportional integral (PI) control would introduce too much variability to the load response, especially with high power loads. Every time there is a small change in the grid frequency, the change would be reflected in the VSD power response. To mitigate this, a wide deadband would have to be used, which limits the benefits to the nadir grid frequency, or a low proportional constant could be used. This would limit the amount of regulation the motor could provide. However, if a set triggered ramp response is used, like the one used in this case, the response can be triggered within a smaller deadband and allow for a larger regulation range.

III. Experimental Results

The proposed frequency regulation is implemented in VSDs and modeled in both a transmission system in EMTDC/PSCAD and verified on the HTB platform. The default power system scale for the Western Electricity Coordinating Council (WECC) power network and the HTB's power and voltage bases are displayed in Table III. The simulations in PSCAD/EMTDC are done in the WECC power and voltage bases. However, when implemented on the HTB platform, all models must be converted to the HTB bases before being sent to the inner current loop control of the HTB's VSIs.

TABLE III. WECC system and HTB: power and voltage bases.

Base	WECC	HTB
Power	10 GVA	2 kW
Voltage	500 kV	43.8 V

A. VSD Model Verification in HTB

The VSD model was verified by comparing the results on the HTB platform and a benchmark simulation for a two bus system. To verify the behavior of the VSD and the frequency regulation on the HTB, it was tested in a single area cabinet. The results show the response of the VSD during frequency regulation on both the HTB platform and the simulation environment. The grid frequency on the HTB platform is shown in the two cases of compensated and uncompensated. In the compensated response, frequency regulation is active in the VSD and responds to the control described in Section II-B. The rate of change for the VSD rotational motor speed is 6 Hz/s. For the uncompensated case, the VSD responds as it would if there was no frequency regulation active.

A constant-impedance, constant-current, and constant-power (ZIP) model is used to represent static load type compared with the performance of the dynamic VSD load. For these examples, the inertia constant, H, for the induction motor is 1 s, which represents a large industrial motor. Fig. 10 shows the simulated and emulated values for the VSD during frequency regulation. This shows that the model on HTB platform is consistent with the benchmark model. Fig. 11 shows the results from the HTB for a ZIP load increase from 0.095 p.u. to 0.3 p.u. with and without frequency regulation compensation. The ZIP load change is significantly larger than the VSD capacity, meaning the frequency cannot return to 60

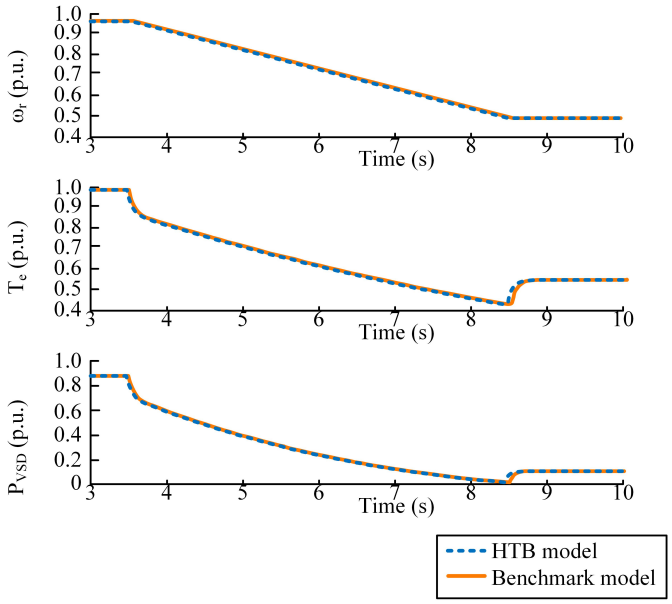

Fig. 10. VSD model response on HTB platform and simulation benchmark model during frequency regulation.

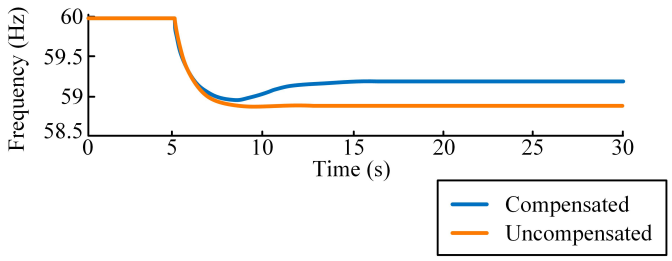

Fig. 11. Grid frequency during real power ZIP load increase on HTB platform with frequency regulation (compensated) and without frequency regulation (uncompensated).

Hz without additional frequency regulation provided by other generation sources or loads in the system.

B. Grid Implementation

The active front end VSD and grid frequency regulation was applied to an aggregate model of the WECC area system, shown in Fig. 12. The system was simulated in EMTDC/PSCAD. All the generators are represented by synchronous generators, and there is a VSD at Bus 10 and Bus 11. The remaining loads are represented as ZIP loads.

High power motors generally have high inertia, which changes the dynamic response of the VSD power. For this case, the inertia constant of the motor is set to $H = 1$ s. Fig. 13 shows the motor and VSD characteristics when the VSD is providing frequency regulation. Each of the graphs are expressed in the per unit value with regard to the WECC system base values, shown in III. Once the grid frequency goes outside the specified deadband, the control begins to ramp the inverter voltage. Due to the V/f control method, this results in the motor speed ramping down at the same rate. Due to the torque speed characteristics of an induction motor, when the motor speed begins to ramp, the motor electrical torque

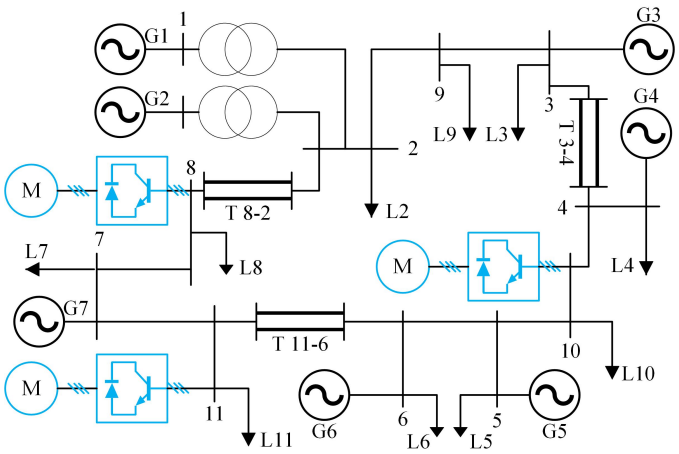

Fig. 12. One line diagram of aggregate model of WECC system.

will decrease, which can be seen at 15 s in Fig. 13. Once the motor speed stops ramping at 50% of its nominal speed, the torque increases, which is shown at 25 s. The behavior happens in reverse once the motor speed begins to ramp to its nominal value, shown at 35 s — the torque initially increases and then decreases once the motor speed ramping has stopped. The torque behavior is then reflected in the DC link current and VSD active power.

In this case, high power motor systems represent roughly 10% of the total load. According to the United States Industrial Electric Motor Systems Market Opportunities Assessment performed in 2002, industrial motor systems above 200 hp make up 44.6% of the total industrial motor energy consumption. According to this same report, industrial motor systems make up 25% of the total energy consumption in the United States [2]. Therefore, it can be estimated that industrial motors above 200 hp make up roughly 11% of the total load on the WECC system, so a 10% penetration is a good representation of the large motors driving a fan, pump, or compressor on the system. There are two aggregate VSD models on the system. For simplification, it is assumed that one model with a larger power consumption can represent multiple smaller systems. Due to the fact that frequency is fairly global for a localized part of the grid, then the frequency control can be accurately represented by one system.

In order to test the response of VSD connected medium voltage induction motors, the value of the inertia constant, H, was set to 1 s for these test cases. This is the commonly accepted value for large induction motors above 200 hp. Automatic generation control (AGC) for frequency is also active in generator 4 and generator 6. AGC activates 4 seconds after the initial frequency event and remains active for the rest of the test case. The frequency response is initiated by adding a ZIP step load that is equal to 10% of the amount of generation at the time of the event.

IV. Discussion

When there is a ZIP load increase near a bus with a VSD, the frequency response throughout the system is improved. Fig. 14 shows that the minimum frequency during the event

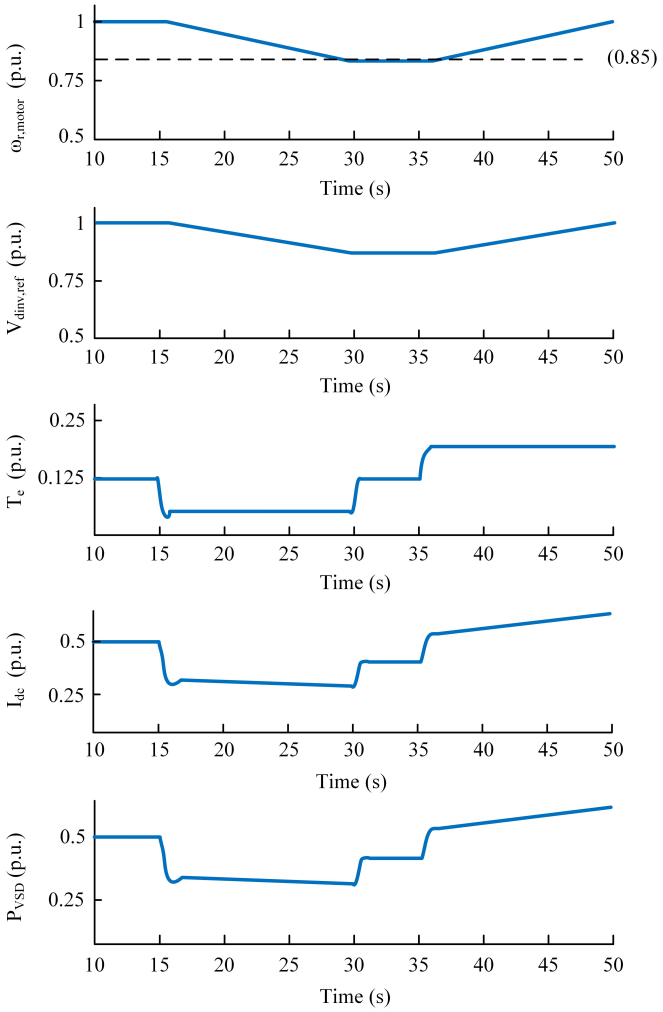

Fig. 13. VSD power and induction motor stator voltage and current for grid frequency regulation on the WECC system.

is reduced at Bus 4 and Bus 6, and the frequency returns to the nominal value of 60 Hz quicker. Fig. 15 shows a similar response, where the ZIP load increase happens at Bus 4. The frequency deviation from the nominal during the event is reduced for Buses 6 and 7. Fig. 16 shows the case where there is a load loss on the system because of the outage of a transmission line that serves a large load center.

Table IV shows the nadir frequencies after the load increase for all the generators on the system. There are three cases shown in the table – a load increase at Bus 4, a load increase at Bus 7, and a load decrease at Bus 4. Percent improvement was found using:

$$PercentImprovement = 100 * \frac{f_{comp} - f_{uncomp}}{60 - f_{uncomp}} \quad (5)$$

You can see from this data that the improvement in the nadir frequency is the greatest the furthest from the event. The nadir frequency at the bus where the event occurred only improved by around 20% for both cases where there was a load added. However, at the buses furthest from the event, the nadir frequency was improved by around 70%. For the case where a load was lost, the greatest improvement was at Generator 6

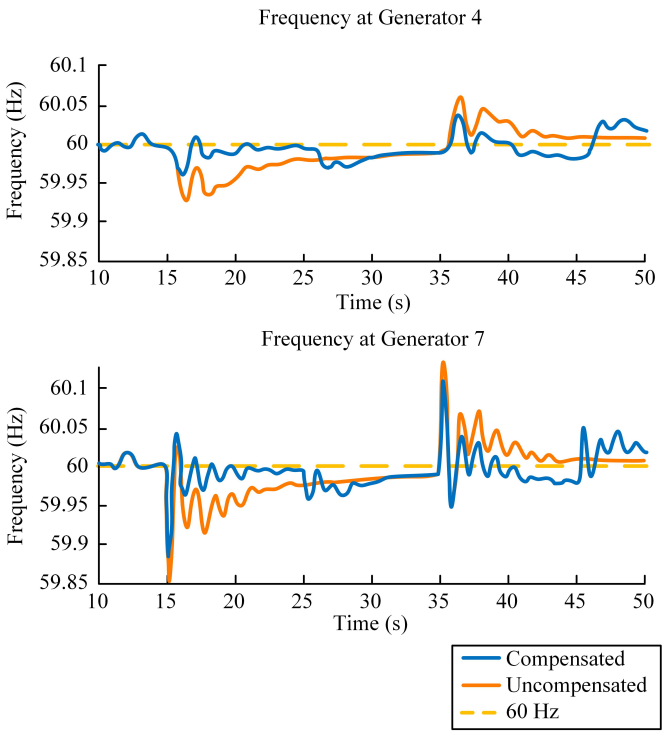

Fig. 14. Frequency of generators 4 and 7 during 530 MW ZIP load increase at Bus 7 comparing with frequency regulation (compensated) and without frequency regulation (uncompensated).

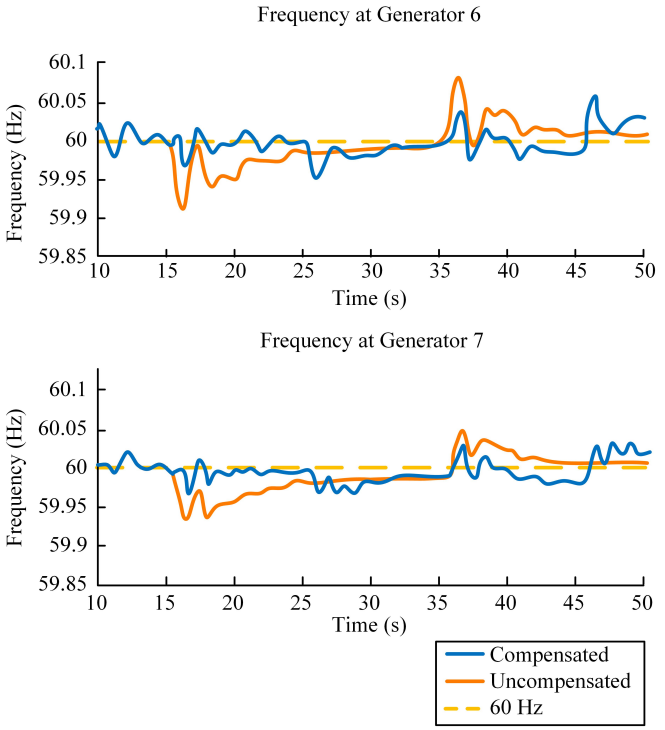

Fig. 15. Frequency of generators 6 and 7 during 485 MW ZIP load increase at Bus 4 comparing with frequency regulation (compensated) and without frequency regulation (uncompensated).

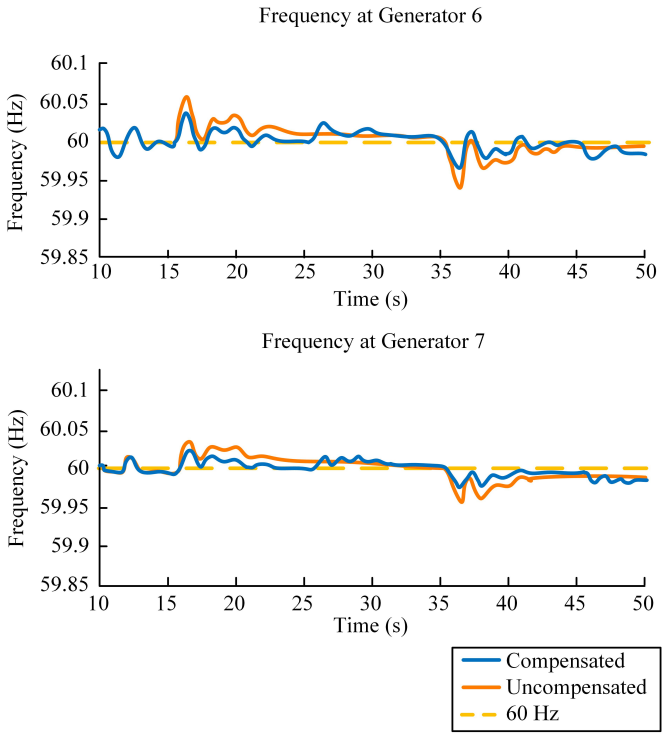

Fig. 16. Frequency of generators 6 and 7 during 360 MW ZIP load loss at Bus 4 comparing with frequency regulation (compensated) and without frequency regulation (uncompensated).

at around 35%. However, there was little improvement in the nadir frequency at Generator 4, which is the bus location of the load loss. This loss of load could be caused by a loss of transmission line on the grid.

While the high inertia loads allow significant improvements to the nadir frequency, is can introduce more variability into the system. The high inertia causes the power to change fairly drastically when the motor is changing speed. When the frequency regulation is first triggered at 15 seconds, this actually can assist the grid in reducing the nadir frequency. However, since the motor speed is limited to only reducing its speed by 50%, the motor speed stops ramping at 25 seconds, causing an additional fluctuation in the power. This fluctuation causes a ripple in the grid frequency. While this ripple still remains lower than then initial nadir frequency without compensation, it still adds variability to the grid frequency. This same effect can be seen after the load event recovers at 35 seconds. The motor speed will ramp until it reaches its nominal value of 60 Hz. When the speed stops ramping, there will be a jump in VSD power to its nominal value.

This paper has evaluated the advantages and disadvantages of implementing a frequency regulation method using an open loop motor drive control. The open loop constant V/f control was chosen because of its cost effectiveness. This limits the additional hardware and control design needed for customers to participate in frequency regulation. With the constant V/f control, a PI frequency regulation, which is commonly used, was determined to bring too much variability to the load. Because even with a broad deadband, the grid

TABLE IV. Nadir frequency for generators during frequency event on WECC system with and without VSD frequency compensation.

Generator	Compensated	Uncompensated	Percent Improvement
Load increase at Bus 4			
Generator 1	59.98 Hz	59.92 Hz	71.00%
Generator 2	59.98 Hz	59.93 Hz	67.98%
Generator 3	59.97 Hz	59.93 Hz	47.14%
Generator 4	59.90 Hz	59.88 Hz	19.11%
Generator 5	59.97 Hz	59.91 Hz	65.23%
Generator 6	59.97 Hz	59.91 Hz	63.53%
Generator 7	59.97 Hz	59.93 Hz	50.89%
Load increase at Bus 7			
Generator 1	59.98 Hz	59.93 Hz	72.05%
Generator 2	59.98 Hz	59.94 Hz	73.92%
Generator 3	59.97 Hz	59.91 Hz	61.91%
Generator 4	59.96 Hz	59.93 Hz	44.61%
Generator 5	59.94 Hz	59.92 Hz	33.50%
Generator 6	59.94 Hz	59.91 Hz	31.73%
Generator 7	59.89 Hz	59.85 Hz	23.32%
Load decrease at Bus 4			
Generator 1	60.04 Hz	60.05 Hz	29.94%
Generator 2	60.03 Hz	60.04 Hz	31.18%
Generator 3	60.04 Hz	60.05 Hz	22.31%
Generator 4	60.07 Hz	60.08 Hz	6.28%
Generator 5	60.04 Hz	60.06 Hz	33.08%
Generator 6	60.04 Hz	60.06 Hz	35.83%
Generator 7	60.03 Hz	60.044 Hz	32.40%

frequency contained too much variability to design a reliable PI controlled frequency regulation. The control shown in Fig. 9 allows for a more predictable load response.

The results show that this control method can help with the initial frequency change, counteracting the generation-load unbalance; however, if the ramping of the motor speed stops before the load recovers, the inertia causes more variability in the system. Ongoing and future research at CURENT include the modeling and the grid frequency support functions of VSD load which is regulated by sophisticated closed loop controller will be investigated, which includes field oriented control (FOC), direct torque control (DTC), and constant slip current control [28]. Additionally, the aggregated performance of multiple VSD loads will also be focused in the following

research, which provides a more realistic representation of multiple VSD loads dynamic performance.

V. Conclusions

Induction motors make up a significant portion of the load on the power grid. While this paper focused on induction motors due to their popularity, this control method could be expanded to other synchronous machines, which also have the capability of implementing VSDs. The implementation of VSDs on induction motors brings not only efficiency savings for customers, but also possible benefits to utility companies, through demand response and ancillary services. Research has been shown to effectively use generators and energy storage for grid frequency regulation. The use of loads to regulate the grid has often been limited to the on or off option.

VSDs are uniquely equipped to participate in the regulation market because of their ability to control the motor load. The motor speed can be varied, unlike most loads, which are either on or off. This paper not only provides a usable VSD model and frequency control for the HTB platform, but analyzed the strengths and drawbacks of implementing a high inertia load side frequency regulation. While this project used the constant V/f control technique because it is often used due to its cost-effectiveness, other more accurate control techniques, such as field oriented control, could be used to mitigate some drawbacks found in this paper.

In this paper, the bandwidth of induction motor drive active front end outer loop PI controller is designed to be relatively slow, and the dynamic transients of the induction motor load variation process is not specifically considered while designing the corresponding controller parameters. The design principle of induction motor drive active front end PI controller considering the influence of motor load will be investigated in the future work.

The aggregate WECC system had the most benefit with high penetration of VSDs on the grid. The ability to prevent the spread of the frequency event could have major benefits on the wide area grid. However, this requires large motors throughout the system to be equipped with VSDs and frequency regulation control.

Using high inertia loads to participate in frequency regulation has advantages and disadvantages. The high inertia can help with the initial frequency drop, counteracting the generation-load unbalance; however, if the ramping of the motor speed stops before the load recovers, the inertia causes more variability in the system. When the VSD begins to ramp its speed back to its nominal value, the inertia causes the motor current to change rapidly. This is reflected in the VSD power, which can cause a change in the grid frequency.

VI. Acknowledgement

This work was partially supported by the Engineering Research Center Program of the National Science Foundation and the Department of Energy under NSF Award Number EEC1041877 and the CURENT Industry Partnership Program. The work was also partially supported by the DOE EERE Office of Advanced Manufacturing Program under DOE Award DE-EE0007304.

References

[1] P. Waide and C. U. Brunner, "Energy-efficiency policy opportunities for electric motor-driven systems," 2011. [Online]. Available: https://www.oecd-ilibrary.org/content/paper/5kgg52gb9gjd-en

[2] XENERGY INC., "United States industrial electric motor systems market opportunities assessment," U.S. DOE, Office of energy efficiency & renewable energy, WA, Tech. Rep., Dec 2002.

[3] S. Kouro, J. Rodriguez, B. Wu, S. Bernet, and M. Perez, "Powering the future of industry: High-power adjustable speed drive topologies," *IEEE Industry Applications Magazine*, vol. 18, no. 4, pp. 26–39, 2012.

[4] H. N. Hickok, "Adjustable speed - a tool for saving energy losses in pumps, fans, blowers, and compressors," *IEEE Transactions on Industry Applications*, vol. IA-21, no. 1, pp. 124–136, 1985.

[5] R. Saidur, N. Rahim, H. Ping, M. Jahirul, S. Mekhilef, and H. H. Masjuki, "Energy and emission analysis for industrial motors in Malaysia," *Energy Policy*, vol. 37, no. 9, pp. 3650–3658, 2009.

[6] E. Mallada, C. Zhao, and S. Low, "Optimal load-side control for frequency regulation in smart grids," *IEEE Transactions on Automatic Control*, vol. 62, no. 12, pp. 6294–6309, 2017.

[7] J. S. Vardakas, N. Zorba, and C. V. Verikoukis, "A survey on demand response programs in smart grids: Pricing methods and optimization algorithms," *IEEE Communications Surveys & Tutorials*, vol. 17, no. 1, pp. 152–178, 2015.

[8] Y. Rebours, "A comprehensive assessment of markets for frequency and voltage control ancillary services," Ph.D. dissertation, University of Manchester, Manchester, March 2009.

[9] H. Hao, B. M. Sanandaji, K. Poolla, and T. L. Vincent, "Frequency regulation from flexible loads: Potential, economics, and implementation," in *American Control Conference*, 2014, pp. 65–72.

[10] R. Walawalkar, S. Fernands, N. Thakur, and K. R. Chevva, "Evolution and current status of demand response (DR) in electricity markets: Insights from PJM and NYISO," *Energy*, vol. 35, no. 4, pp. 1553–1560, 2010.

[11] J. H. Eto, J. Undrill, C. Roberts, P. Mackin, and J. Ellis, "Frequency control requirements for reliable interconnection frequency response," *Lawrence Berkeley National Laboratory*, 2018, Report: LBNL-2001103.

[12] R. Azizipanah-Abarghooee and M. Malekpour, "Smart induction motor variable frequency drives for primary frequency regulation," *IEEE Transactions on Energy Conversion*, vol. 35, no. 1, pp. 1–10, 2020.

[13] M. Malekpour, R. Azizipanah-Abarghooee, F. Teng, G. Strbac, and V. Terzija, "Fast frequency response from smart induction motor variable speed drives," *IEEE Transactions on Power Systems*, vol. 35, no. 2, pp. 997–1008, 2020.

[14] S. Wang, S. Zhang, Y. Ma, F. Wang, and L. M. Tolbert, "Analysis of MTDC inertia emulation impact on connected AC systems," in *IEEE Energy Conversion Congress and Exposition*, 2018, pp. 3705–3712.

[15] L. M. Tolbert, F. Wang, K. Tomsovic, K. Sun, J. Wang, Y. Ma, and Y. Liu, "Reconfigurable real-time power grid emulator for systems with high penetration of renewables," *IEEE Open Access Journal of Power and Energy*, vol. 7, pp. 489–500, 2020.

[16] S. Zhang, B. Liu, S. Zheng, Y. Ma, F. Wang, and L. M. Tolbert, "Three-phase short-circuit fault implementation in converter based transmission line emulator," in *IEEE Energy Conversion Congress and Exposition*, 2017, pp. 2914–2920.

[17] S. Zhang, B. Liu, S. Zheng, Y. Ma, F. Wang, and L. M. Tolbert, "Development of a converter-based transmission line emulator with three-phase short-circuit fault emulation capability," *IEEE Transactions on Power Electronics*, vol. 33, no. 12, pp. 10 215–10 228, 2018.

[18] L. Yang, Y. Ma, J. Wang, J. Wang, X. Zhang, L. M. Tolbert, F. Wang, and K. Tomsovic, "Three-phase power converter based real-time synchronous generator emulation," *IEEE Transactions on Power Electronics*, vol. 32, no. 2, pp. 1651–1665, Feb. 2017.

[19] J. Wang, L. Yang, Y. Ma, J. Wang, L. M. Tolbert, F. Wang, and K. Tomsovic, "Static and dynamic power system load emulation in converter-based reconfigurable power grid emulator," *IEEE Transactions on Power Electronics*, vol. 31, no. 4, pp. 3239–3251, April 2016.

[20] J. Wang, Y. Ma, L. Yang, L. M. Tolbert, and F. Wang, "Power converter-based three-phase induction motor load emulator," in *IEEE Applied Power Electronics Conference and Exposition*, 2013, pp. 3270–3274.

[21] M. Fioretto, G. Raimondo, L. Rubino, N. Serbia, and P. Marino, "Power losses analysis in AC/DC conversion based on active front end systems," in *International Symposium on Power Electronics, Electrical Drives, Automation and Motion*, 2010, pp. 210–215.

[22] L. Moran, J. Espinoza, M. Ortiz, J. Rodriguez, and J. Dixon, "Practical problems associated with the operation of ASDs based on active

front end converters in power distribution systems," in *IEEE Industry Applications Conference*, 2004, pp. 2568–2572.
[23] L. Wei, Y. Patel, and C. S. N. Murthy, "Evaluation of LCL filter inductor and active front end rectifier losses under different PWM method," in *IEEE Energy Conversion Congress and Exposition*, 2013, pp. 3019–3026.
[24] P. Krause, O. Wasynczuk, S. Sudoff, and S. Pekarek, *Analysis of Electric Machinery and Drive Systems*. Wiley, 2013.
[25] S. Hiti, "Modeling and control of three-phase PWM converters," Ph.D. dissertation, Virginia Polytechnic Institute and State University, Blacksburg, Virginia, July 1995.
[26] P. Verdelho and G. D. Marques, "DC voltage control and stability analysis of PWM-voltage-type reversible rectifiers," *IEEE Transactions on Industrial Electronics*, vol. 45, no. 2, pp. 263–273, 1998.
[27] B. Akin and N. Garg. (2013, July) Scalar (V/f) control of 3-phase induction motors. [Online]. Available: https://www.ti.com/lit/an/sprabq8/sprabq8.pdf
[28] S. Wang, Y. Ma, T. Short, L. M. Tolbert, and F. Wang, "Power emulator of variable speed drive with grid frequency support in multi-converter based power grid emulation system," in *IEEE Energy Conversion Congress and Exposition*, Oct. 11-15, 2020, pp. 1694–1701.

Taylor Short received both her B.S. (2018) and M.S. (2020) in electrical engineering from the University of Tennessee in Knoxville, TN. During her time at the University of Tennessee, she participated in research for the Center for Ultra-Wide-Area Resilient Electric Energy Transmission Networks (CURENT). She is now pursuing a PhD at The Ohio State University in engineering education.

Shuyao Wang received her B.S. and M.S. degree in electrical engineering from North China Electric Power University, Beijing, in 2013 and 2016 respectively. She has been working towards her Ph.D. degree in electrical engineering in the University of Tennessee, Knoxville since 2016. Her research interests are related to modular multi-level converters, HVDC transmission system, power grid ancillary services, and power electronics based devices modeling.

Leon M. Tolbert (Fellow, IEEE) received the bachelor's, M.S., and Ph.D. degrees in electrical engineering from the Georgia Institute of Technology, Atlanta, in 1989, 1991, and 1999, respectively. He is currently a Chancellor's Professor and the Min H. Kao Professor with the Department of Electrical Engineering and Computer Science, The University of Tennessee. He is a founding member for the NSF/DOE Engineering Research Center, CURENT (Center for Ultra-wide-area Resilient Electric Energy Transmission Networks). He is also an Adjunct Participant with Oak Ridge National Laboratory. Dr. Tolbert is a Registered Professional Engineer with the State of Tennessee. His research interests include the utility applications of power electronics, microgrids, electric vehicles, and wide bandgap semiconductors.

Jingxin Wang (Member, IEEE) received the B.S. and M.S. degrees from the China University of Mining and Technology, Jiangsu, China, and the Ph.D. degree from Shanghai Jiaotong University, in 2003, 2006, and 2011, respectively, all in electrical engineering. He is currently working as a Research Associate with The University of Tennessee, Knoxville, TN, USA. His research interests include high performance motor control, three-phase converter design, power flow control, and renewable energy.

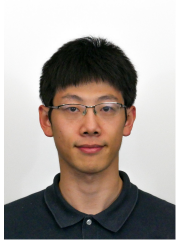

Yiwei Ma (Member, IEEE) received the B.S. and M.S. degrees in electrical engineering from Tsinghua University, Beijing, China, in 2009 and 2011, respectively, and the Ph.D. in electrical engineering from the University of Tennessee, Knoxville, in 2019. Dr. Ma presently is a research engineer at Electric Power Research Institute (EPRI) at their Knoxville, Tennessee, office. His research interests include modeling and control of power electronics interfacing converters for the renewable energy sources, multilevel converters, and microgrids.

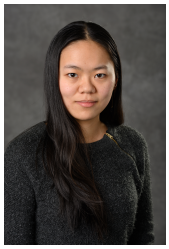

Yunting Liu (Member, IEEE) received the B.S. degree in electrical engineering from Huazhong University of Science and Technology, Wuhan, China, in 2013, and the Ph.D. degree in electrical engineering from Michigan State University, Michigan, USA in 2019. She joined University of Tennessee, Knoxville, as a Post-Doctoral Research Associate in 2019. Her research interests include renewable energy integration, modular multilevel converters, solid-state variable capacitors, and dual-active-bridge dc-dc converters.

Fred (Fei) Wang (Fellow, IEEE) received the B.S. degree from Xi'an Jiaotong University, Xi'an, China, and the M.S. and Ph.D. degrees from the University of Southern California, Los Angeles, CA, USA, in 1982, 1985, and 1990, respectively, all in electrical engineering. Since 2009, he has been with The University of Tennessee and Oak Ridge National Laboratory, Knoxville, TN, USA, as a Professor and the Condra Chair of Excellence in Power Electronics. He is currently a Founding Member and the Technical Director of the Multi-University NSF/DOE Engineering Research Center for Ultra-Wide-Area Resilient Electric Energy Transmission Networks (CURENT) led by The University of Tennessee. His research interests include power electronics, power systems, controls, electric machines, and motor drives.